Mon. Not. R. Astron. Soc. **000**, 000–000 (0000) Printed 1 February 2008 (MN LATEX style file v1.4)

PDS 456: an Extreme Accretion Rate Quasar?

J.N. Reeves[1], P.T. O'Brien[1], S. Vaughan[1], D. Law-Green[1], M. Ward[1], C. Simpson[2], K.A. Pounds[1], R. Edelson[1,3]

[1] *X-Ray Astronomy Group; Department of Physics and Astronomy; Leicester University; Leicester LE1 7RH; U.K.*
[2] *Subaru Telescope, National Astronomical Observatory of Japan, 650 N. A'ohōkū Place, Hilo, HI 96720, U.S.A.*
[3] *Department of Physics and Astronomy; University of California, Los Angeles; Los Angeles, CA 90095-1562; U.S.A.*

1 February 2008

ABSTRACT

We present quasi-simultaneous *ASCA* and *RXTE* observations of the most luminous known AGN in the local (z < 0.3) universe, the recently discovered quasar PDS 456. Multiwavelength observations have been conducted which show that PDS 456 has a bolometric luminosity of $\sim 10^{47}$ erg s^{-1} peaking in the UV part of the spectrum. In the X-ray band the 2-10 keV (rest-frame) luminosity is 10^{45} erg s^{-1}. The broad-band X-ray spectrum obtained with *ASCA* and *RXTE* contains considerable complexity. The most striking feature observed is a very deep, ionised iron K edge, observed at 8.7 keV in the quasar rest-frame. We find that these features are consistent with reprocessing from highly ionised matter, probably the inner accretion disk. PDS 456 appeared to show a strong (factor of ∼2.1) outburst in just ∼17 ksec, although non-intrinsic sources cannot be completely ruled out. If confirmed, this would be an unusual event for such a high-luminosity source, with a light-crossing-time corresponding to $\sim 2R_S$. The implication would be that flaring occurs within the very central regions, or else that PDS 456 is a 'super-Eddington' or relativistically beamed system. Overall we conclude on the basis of the extreme blue/UV luminosity, the rapid X-ray variability and from the imprint of highly ionised material on the X-ray spectrum, that PDS 456 is a quasar with an unusually high accretion rate.

Key words: galaxies: active – quasars: individual: PDS 456 – X-rays: quasars

1 INTRODUCTION

Understanding the origin of the luminous, ionising continuum from Active Galactic Nuclei (AGN) is one of the prime goals of AGN research. Despite the general acceptance of the standard AGN paradigm — that the continuum (UV) emission originates in an accretion disk around a super-massive black hole — the details remain unclear. In the X-ray band, there is a hard power-law component that dominates above 2 keV in the well studied Seyfert 1 galaxies. This hard X-ray continuum may originate from a hot corona above the surface of the accretion disk, in which optical/UV photons from the disk are Comptonised to X-ray energies. These X-rays then illuminate the disk, being either 'reflected' towards the observer or thermalised back into optical/UV emission. In the X-ray spectral band, evidence for this disk reflection component is seen in the form of a fluorescent Fe Kα line at 6.4 keV, an iron K edge at > 7 keV and a Compton 'hard tail'. All these features have been observed in Seyfert 1 galaxies (e.g. Pounds et al. 1990, Nandra & Pounds 1994).

The subject of this paper is the recently discovered *radio-quiet* quasar PDS 456 (Torres et al. 1997, Simpson et al. 1999), which is *the* most luminous known object in the local Universe (z < 0.3); indeed the bolometric luminosity of PDS 456 exceeds that of the well-known radio-loud quasar 3C 273. However, unlike 3C 273, PDS 456 is radio-quiet, and thus presumably not jet dominated. Therefore, PDS 456 provides a unique opportunity to study in detail the hard and soft X-ray components in a high luminosity, radio-quiet AGN, and in particular to test models of reflection expected from the putative accretion disk.

In the next section we describe the multi-wavelength properties of PDS 456. The main subject of this paper is then covered; the X-ray emission from PDS 456, using observations with *ASCA* and *RXTE*. Values of $H_0 = 50$ km s^{-1} Mpc^{-1} and $q_0 = 0.5$ have been assumed throughout and all fit parameters are given in the quasar rest-frame. Note that errors are in this paper are quoted at the 90% confidence level (e.g. $\Delta\chi^2 = 2.7$ for one interesting parameter).

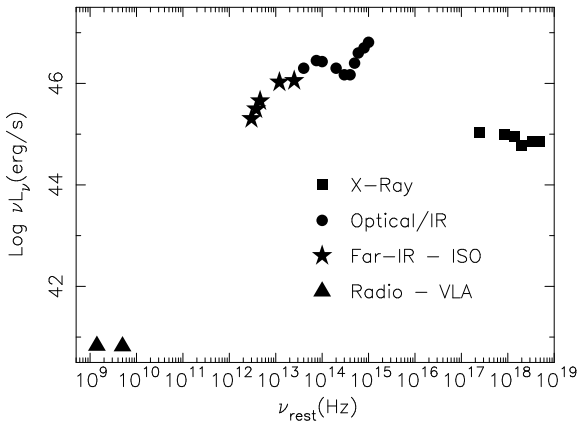

Figure 1. The radio to X-ray SED of the quasar PDS 456. X-ray (ROSAT, ASCA, RXTE), infra-red (ISO) and radio (VLA) data are plotted; the dereddened optical/near-IR data has been taken from Simpson et al. (1999). It is seen that the bolometric luminosity of PDS 456 approaches 10^{47} erg s^{-1}.

2 MULTIWAVELENGTH PROPERTIES OF PDS 456

At $z = 0.184$, PDS 456 has a de-reddened, absolute blue magnitude $M_B \approx -27$, making it more luminous than the radio-loud quasar 3C 273 ($z = 0.158$, $M_B \approx -26$). The Galactic absorption column towards PDS 456 is 2.4×10^{21} cm^{-2} (Stark et al. 1992), with an extinction of $A_V = 1.4$ in the optical. We have performed a recent VLA observation; the total detected 6 cm flux of 8 mJy confirms that PDS 456 is radio-quiet ($R_L = \log[F_{6cm}/F_B] \approx$ -0.74). PDS 456 has broad Balmer and Paschen lines, strong Fe II, a hard (de-reddened) optical continuum ($f_\nu \propto \nu^{-0.1\pm0.1}$), and one of the strongest 'big blue bumps' of any AGN (Simpson et al. 1999). PDS 456 is coincident (to $< 10''$) with the *ROSAT* soft X-ray source RXS J172819.3-141600 (Voges *et al.* 1999); the count rate is 0.30 ± 0.02 ct/s corresponding to $L_X \sim 10^{45}$ erg s^{-1}. The overall spectral energy distribution of PDS 456 (figure 1), obtained from all our current data on this quasar (including recent VLA and ISO data, listed in table 1), gives a bolometric luminosity of $\sim 10^{47}$erg s^{-1}, a value more typical of QSOs at $z \sim 3$.

3 X-RAY OBSERVATIONS AND DATA REDUCTION

3.1 ASCA observations

PDS 456 was observed by *ASCA* on 7–8 March 1998 with a total duration of ∼140 ks. Standard screening criteria were applied to the *ASCA* data (e.g. see the *ASCA Data Reduction Guide*), giving a total 'good' exposure time of ∼ 40 ksec per detector. Counts were extracted using a $4'$ circular aperture centered on the source, and the background was estimated using source-free regions at similar off-axis angles.

3.2 RXTE observations

PDS 456 was observed by *RXTE* on 7-10 March 1998 with a total duration of 226 ks. We extracted STANDARD-2 data from the PCU (Proportional Counter Unit) array using the REX reduction script supplied by NASA/GSFC. Data have been extracted from Layer 1 (L1) only (the first and most sensitive layer). Poor quality data were excluded on the basis of the following selection criteria: (i) the satellite is out of the South Atlantic Anomaly (SAA); (ii) Earth elevation angle $\geq 10°$; (iii) offset from the optical position of PDS 456 is $\leq 0.02°$; and finally (iv) ELECTRON-0$\leq$ 0.1. This last criterion removes data with high anti-coincidence rate in the PCUs. The total 'good' exposure time selected after this screening was 92 ksec. The background was estimated using the L7-240 model. All *RXTE* spectral data below 2.5 keV and above 18 keV have been ignored.

Table 1. ISO (ISOPHOT) and VLA fluxes.

ISO Data		VLA Data	
$\lambda(\mu$m)	Flux(Jy)	ν(Hz)	Flux(mJy)
12	0.28 ± 0.03	1.4	30.4
25	0.55 ± 0.12	4.85	8.23
50	0.61 ± 0.11		
80	0.51 ± 0.11		
100	0.42 ± 0.14		

4 SPECTRAL ANALYSIS

Initially the hard X-ray (*RXTE*+*ASCA*) data in the 2.5-18 keV range were analysed, using background subtracted spectra and by allowing the relative normalisations of all 5 instruments to vary. The pulse height spectra from each detector were binned to give at least 20 counts per spectral channel. Firstly, a power-law plus fixed Galactic absorption (model 1) gives a poor fit ($\chi^2_\nu = 1.62$) to the data (see Table 2 for a summary of the model fits). Clear deviations in the data–model residuals are present around the iron K-shell regime, both in the *ASCA* and particularly the *RXTE* data (see figure 2). We therefore added an iron K edge and line to the fits, to model the effects of Compton reflection off the accretion disk, as observed in many Seyfert 1s (e.g. Pounds et al. 1990). We first considered a neutral (but narrow; $\sigma =$ 0.01 keV) iron line and edge (model 2) fixed at 6.4 and 7.1 keV respectively. Although there is some improvement in the model fits, the overall fit remained unacceptable. A further improvement was obtained using a broad Fe line (model 3), although the fit was still inadequate as an edge was apparent in the data residuals at > 7 keV. The derived line strength is rather high (EW ∼ 900 eV); the line is also unusually broad ($\sigma \sim 1.4$ keV) and redshifted (E ∼ 5.6 keV).

We next tried a fit to highly ionised iron (model 4), the (narrow) line energy was fixed at 6.7 keV (corresponding to He-like Fe) and the edge energy was left as a free parameter. In this case an acceptable fit was found to the data ($\chi^2_\nu \approx 1$); with a deep and highly ionised iron K edge at 8.7 keV with $\tau = 0.76 \pm 0.12$. A *narrow* iron emission line was no longer required in the fit (EW$<$ 77 eV). The energy of the edge is consistent with iron of ionisation from Fe XXIII – Fe XXV. Figure 3 clearly illustrates the high ionisation state of the reprocessing material. Note that we also tried fitting a smeared edge model (width 1 keV), as might be expected from the inner disk, although the fit obtained was very similar to above. Including a *broad* iron line in the

Table 2. Results of simultaneous spectral fits to the *ASCA* and *RXTE* data in the 2.5–18 keV range. Column 1 gives the models as defined in the text. Columns 2–7 give the fit parameters: column 2 gives the power law photon index; column 3 the iron K edge energy (keV) or ionization parameter (ξ); column 4 gives the edge depth (τ), reflection strength (R= $\Omega/2\pi$) or N_H (units 10^{22} cm^{-2}). Columns 5, 6 and 7 give the iron K line energy (keV), the intrinsic width σ (in keV) and equivalent width (in eV) respectively. Column 8 gives the best-fit χ^2 over number of degrees of freedom. ^{f} indicates the parameter is fixed.

Model	Γ	E_{edge} or ξ	τ, R or N_H	E_{line}	σ	EW	χ^2/dof
(1)	(2)	(3)	(4)	(5)	(6)	(7)	(8)
1. PL	2.38±0.03	–	–	–	–	–	343/212
2. PL+LINE	2.42±0.04	7.1^f	< 0.10	6.4^f	0.01^f	178±49	309/210
3. PL+BROAD-LINE	2.44±0.05	–	–	$5.6^{+0.5}_{-0.6}$	$1.4^{+0.5}_{-0.4}$	900^{+650}_{-300}	230/209
4. PL+EDGE+LINE	2.12±0.04	8.70±0.15	0.76±0.12	6.7^f	0.01^f	< 77	211/209
5. PL+EDGE+B-LINE	2.22±0.08	8.7±0.3	0.53±0.18	6.1±0.5	$1.2^{+0.8}_{-0.7}$	340^{+410}_{-200}	200/207
6. PL+PEXRIV+LINE	2.54±0.07	6400^{+2650}_{-2350}	$0.92^{+0.39}_{-0.27}$	6.7^f	0.01^f	< 30	207/209
7. PL+ABSORI+LINE	2.39±0.08	$1.5^{+0.6}_{-0.4} \times 10^4$	47^{+16}_{-11}	6.7^f	0.01^f	< 35	199/209

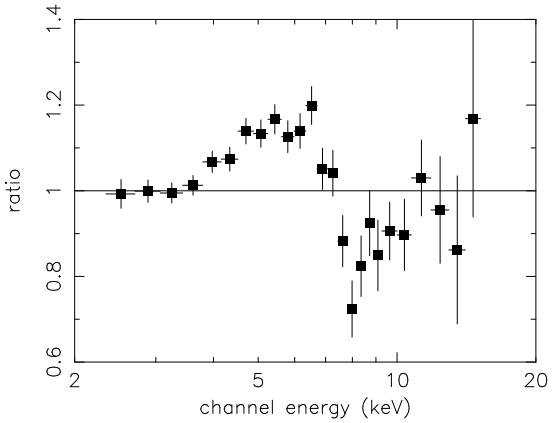

Figure 2. The data/model ratio residuals from a simple power-law fit fit (model 1) to the *RXTE* data of PDS 456. The effect of the deep, ionised iron K edge is clearly seen in the residuals.

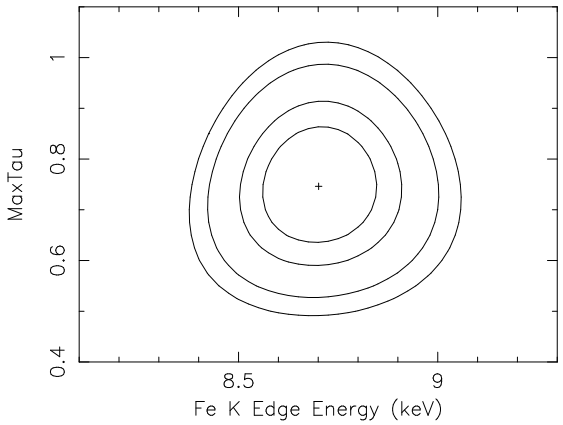

Figure 3. Confidence contours of Fe K edge energy against depth, for the *RXTE* and *ASCA* spectrum of PDS 456. The contours represent the 68%, 90%, 99%, 99.9% significance levels respectively.

model (in addition to the edge, model 5) lead to a further improvement in the spectral fit ($\Delta\chi^2 \sim 11$), at a significance level of $\sim 99\%$ confidence (F-test, 2 additional parameters). The line equivalent width is $\sim$ 350 eV; the line is broad ($\sigma \sim 1$ keV) and possibly redshifted (E $\sim$ 6 keV). We note that the detection of the ionised iron edge is robust, even after the inclusion of a broad line in the model fit.

Having established the presence of reprocessing by highly ionised matter, we then attempted to model these reprocessing features in terms of reflection of X-rays off the surface layers of an ionised accretion disk. The PEXRIV model in XSPEC was used (Magdziarz & Zdziarski 1995), assuming a disk surface temperature of 10^6 K (e.g. Zycki et al. 1994; Ross, Fabian & Young 1999) and a disk inclination angle of 30°. The disk ionisation parameter (ξ) and the strength of the reflection component R (=$\Omega/2\pi$) were both left as free parameters in the fit. (Note that $\xi = L/nr^2$, where n is the number density of the material at a distance r from an ionising source of luminosity L, where L is defined from 5 eV to 20 keV.) An ionised reflector provided a good fit to the hard X-ray spectrum and the iron K edge (model 6, $\chi^2_\nu \approx 1$), giving a value of R close to 1 and a high ionisation (ξ = 6400 erg cm s^{-1}). Although a narrow iron K line is not required in this fit, the presence of a broad line was not ruled out (EW $\lesssim$ 250 eV).

We also attempt to model the hard X-ray spectrum of PDS 456 with a power-law modified by a warm line-of-sight absorber (model 7), using the ABSORI routine in XSPEC (note we assume a temperature of $T = 3 \times 10^5$ K). This model provides a good alternative description of the X-ray data, modelling both the ionised edge and providing a good overall fit ($\chi^2_\nu \approx 1$). However both a large column of material ($N_H \approx 4.7 \times 10^{23}$ cm^{-2}) and a very high degree of ionisation ($\xi = 1.5 \times 10^4$ erg cm s^{-1}) are required to reproduce the energy and depth of the edge feature.

Extrapolation of the preferred hard X-ray spectral model to lower energies (0.7 keV) does not provide an adequate description of the broad-band data. There remains a significant deficit of counts present below ∼2 keV (see figure 4, panel 1), indicating that significant intrinsic absorption (in excess of Galactic) is present. A neutral absorber ($N_{\rm H} \sim 10^{22}$cm^{-2}) gave a poor fit; the spectrum is poorly modelled and an excess of counts is present below 1 keV in the *ASCA* data. However an *ionised* absorber provides a good fit (figure 4, panel 2), with $N_{\rm H} \sim 5 \pm 1.5 \times 10^{22}$cm^{-2} and $\xi \sim 350 \pm 100$ (again assuming T = 3×10^5 K). Note that this material is not sufficiently ionised to reproduce the deep, ionised, iron K edge seen in the hard X-ray spectrum; the absorber effectively contributes a negligible amount ($\tau < 0.1$)

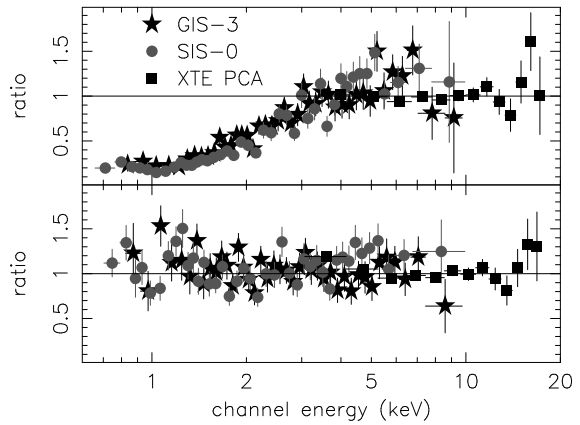

Figure 4. Data-ratio residuals for the broadband 0.7-18 keV *ASCA* and *RXTE* spectrum of PDS 456. The first panel shows the hard X-ray spectrum extrapolated down to lower energies. The deficit of counts below 2 keV indicates the presence of substantial soft X-ray absorption. The lower panel shows the data residuals, after including a warm absorber of column $\sim 5 \times 10^{22}\mathrm{cm}^{-2}$.

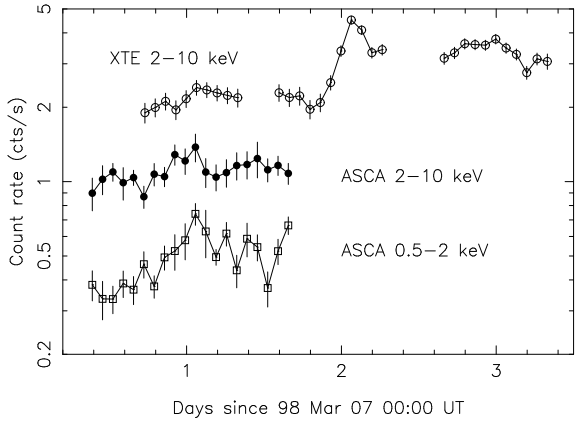

Figure 5. *RXTE* and *ASCA* light curves for PDS 456. The *ASCA* data were shifted upwards in this logarithmic plot by an arbitrary amount and the errors on the *RXTE* data were increased by 0.15 ct/s in quadrature to account for systematic errors. The source appears to flare by a factor of ∼2.1 in 17 ksec, corresponding to a light-crossing size of $\sim 2R_S$.

to the iron K edge. The absence of any appreciable optical absorption (aside from Galactic) may also imply either a low intrinsic dust-to-gas ratio, or that most of the dust close to the central engine has sublimated.

5 TEMPORAL ANALYSIS

Light curves were constructed by binning the data into 96 min orbital bins, for the background-subtracted *RXTE* (2–10 keV) and *ASCA* (2–10 and 0.5–2 keV) data. The results are plotted in Figure 5. The *RXTE* light curve shows an increase by a factor of ∼2.1 in 3 orbits (17 ksec). Note that the time-averaged *RXTE* flux in the 2-10 keV band is 8.5×10^{-12} erg cm^{-2} s^{-1}, and if this flare is real, it would be the most rapid variation ever seen in a radio-quiet quasar. Unfortunately the (lower signal/noise) *ASCA* observation had ended before the flare began, so independent confirmation is not possible. In order to assess the reality of this event, we consider two possibilities that arise because *RXTE* is a non-imaging instrument: 1) the flare could be due to an error in the background subtraction, and 2) it could be due to variations in a contaminating source in the *RXTE* beam.

Figure 6 shows the derived on source data (2–10 keV L1) along with two estimators of the background residuals (2–10 keV Layer 2 [L2], and 20–40 keV Layer 1 [L1]). The background model was determined in the same fashion for all three light curves. As X-rays from this rather weak source should not contribute significantly to the 2–10 keV L2 and 20–40 keV L1 count rates, these residuals can be used to assess the quality of the background subtraction. The 2–10 keV L2 data are well-behaved, consistent with the estimated 0.15 ct/s systematic error, but the 20–40 keV L1 show apparently small periodic daily excursions on the ∼0.5 ct/s level. These latter excursions are not correlated with the flare, but instead look like errors in modelling the daily effect of SAA passage. Thus, we consider it unlikely that the observed flare could be due entirely to poor background subtraction.

No contaminating sources of sufficient brightness were seen in the *ASCA* image, but that covered only ∼20% of the $\sim 1^o$ *RXTE* field-of-view. The RASSBSC (Voges et al. 1996) was searched and no sources were found within 1^o of PDS 456. *Ginga* background fluctuation data (Butcher et al. 1997), which do cover a similar energy band, suggest a $\lesssim$2% probability of a contaminating source at the 2 ct/s level; a similar probability of 2.5% is found from the distribution of Piccinotti et al. (1982). However, there is no assurance that the *RXTE* field-of-view does not contain a highly variable contaminating source at a lower flux level. For instance, the Butcher et al. data suggest that a few sources could be expected with mean *RXTE* count rates of 0.2–0.4 ct/s. If one of these is a narrow-line Seyfert 1 galaxy (NLS1s can show factor of $\gtrsim$5 in a few hours; e.g., Boller, Brandt & Fink 1996), or even a BL-Lac object, this could produce a spurious flare identical to the one seen. This is unlikely but cannot be ruled out. Thus the most likely interpretation of the data is that the flare is intrinsic to PDS 456, but other possibilities cannot be completely excluded. The discussion below assumes that the flare is intrinsic to the QSO.

6 DISCUSSION

We find that PDS 456 has an unusual X-ray spectrum, with a deep, highly ionised iron K edge and a broad (but poorly constrained) iron line, superimposed on a steep hard X-ray continuum. Lower energy residuals, corresponding to a warm absorber also seem to be present in the soft X-ray band. The high energy iron K features arise from a highly ionised reprocessor. One possibility is through Compton reflection of hard X-rays off a high ionisation accretion disk. An alternative model involves reprocessing from line-of-sight matter (a 'warm absorber'). However, in the latter case, the degree of ionisation required to produce such a deep and highly ionised edge seems rather high when compared to the warm absorbers observed in Seyfert 1s (Reynolds 1997); indeed it

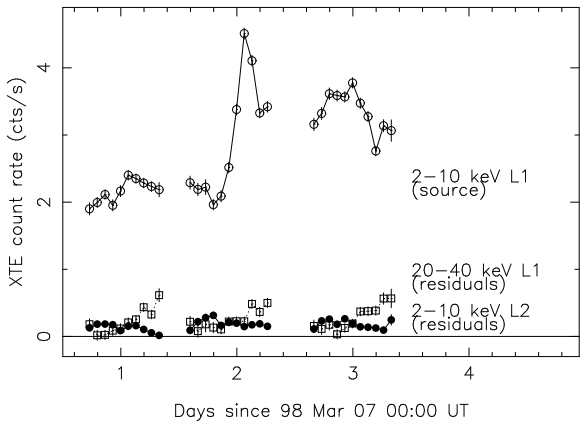

Figure 6. Background-subtracted on-source (2–10 keV L1) and residual (2–10 keV L2 and 20–40 keV L1) light curves, plotted on a linear scale, with no systematic errors included.

is possible that such a high ionisation absorber may not be thermally stable (see Reynolds & Fabian 1995).

Overall an ionised reflector appears a more physically appealing description of the hard X-ray data. Indeed strong, highly ionised, iron-K edge features are predicted by disk photoionisation models (e.g. Ross, Fabian & Young 1999) and are also thought to be observed in some high-state Galactic black-hole candidates (e.g. Zycki, Done & Smith 1997). The iron line and edge produced in such highly ionised disks can be significantly broadened through multiple Compton scatterings (e.g. Ross et al. 1999). However we were unable to differentiate here between a smeared and a sharp iron edge, given the limited signal to noise of our observations.

The high ionisation of the reflector could imply a high accretion rate in PDS 456 (relative to the Eddington limit), particularly as $\xi \propto \dot{m}^3$ in a photoionised accretion disk (e.g. Matt, Fabian & Ross 1993). This interpretation is consistent with the other X-ray properties of PDS 456, namely a steep underlying continuum and rapid X-ray variability, both of which are commonplace in NLS1s (Vaughan et al. 1999a and references therein). NLS1s are also thought to be accreting near the Eddington limit (e.g. Pounds, Done & Osborne 1995); indeed recent evidence has been found in one NLS1 (Ark 564) for a spectrum consistent with ionised disk reflection (Vaughan et al. 1999b). Ionised iron line features have also been observed in other luminous radio-quiet quasars (Reeves et al. 1997; Nandra et al. 1997). An unusually high accretion rate may even account for the complete lack of X-ray spectral features in some of the most luminous quasars (Nandra et al. 1995, Reeves & Turner 1999). However PDS 456 seems to provide the clearest example for the presence of ionised iron features in a high luminosity AGN.

The one obvious flare in the X-ray light curve (figure 5) has a doubling time of ∼15 ks. This suggests, from simple light-crossing arguments, a maximum size of $l = 4.5\times10^{12}$ m for the varying region. For a black hole of mass $10^9 M_\odot$ (corresponding to PDS 456, with $L_{BOL} = 10^{47}$ erg s^{-1}, at the Eddington limit), this implies that the X-ray flare occurs within a region of less than 2 Schwarzschild radii ($2R_S$). (A more conservative H_0 of 75 km s^{-1} Mpc^{-1} gives a region of $< 5R_S$, which is still tightly constrained). A smaller mass black hole would loosen this requirement somewhat, but would then imply a super-Eddington accretion rate. *Therefore one possible implication of the rapid variability is accretion near to or greater than L_{Edd}.* The variability also implies a (non-beamed) efficiency of converting matter to energy of ∼ 5%, close to the limit for a Schwarzschild black hole (see Fabian 1979). Some Seyfert 1s (such as MCG-6-30-15, Reynolds et al. 1995) can also exhibit rapid variability, limiting the X-ray emission to a few R_S. Rapid flux changes have also been reported in 2 narrow-line QSOs; in PKS 0558-504, a 70% increase is observed in 3 minutes (Remillard et al. 1991) and PHL 1092 shows a reported increase by a factor of 3.8, using the *ROSAT* HRI, in less than 5000 sec (Brandt et al. 1999). In any event, the flare in PDS 456 must come from a very compact region (for instance, a small hot spot on the disk), presumably very close to the "central engine" in which the luminosity is actually generated.

In conclusion PDS 456 is a remarkable object, showing clear features of a high ionisation reprocessor, one possible interpretation of which is through reflection off a highly ionised accretion disk. Both the high ionisation spectral features and the extreme rapid variability suggest that the super-massive black hole in PDS 456 could be running at an unusually high accretion rate.

REFERENCES

Boller, Th., Brandt, W. N. & Fink, H., 1996, A&A, 305, 53
Brandt, W.N., Boller, Th., Fabian, A.C., Ruszkowski, M., 1999, MNRAS, 303, 53L
Butcher, J. et 1997, MNRAS, 291, 437
Fabian, A.C., 1979, Proc. R.Soc London., Ser A, 336, 449
Magdziarz, P., Zdziarski, A. A. 1995, MNRAS, 273, 837
Matt, G., Fabian, A.C., Ross, R.R., 1993, MNRAS, 262, 179
Nandra, K., George, I.M., Mushotzky, R.F., Turner, T.J., Yaqoob, T., 1997, ApJ, 488, L91
Nandra K., *et al.* 1995, MNRAS, 276, 1
Nandra, K., Pounds K. A., 1994, MNRAS, 268, 405
Piccinotti, G. et al. ApJ, 1982, 253, 485
Pounds, K.A., Done, C. Osborne, J.P., 1995. MNRAS, 277, L5.
Pounds, K.A., Nandra, K., Stewart, G.C., George, I.M., Fabian, A.C., 1990, Nature, 344, 132
Reeves, J.N., Turner, M.J.L., 1999, MNRAS, submitted
Reeves, J.N., Turner, M.J.L., Ohashi, T. and Kii, T., 1997, MNRAS, 292, 468
Remillard, R.A., Grossan, B., Bradt, H.V., Ohashi, T., Hayashida, K., 1991, Nature, 350, 589
Reynolds, C.S, 1997, MNRAS, 286, 513
Reynolds, C.S., Fabian, A.C., Nandra, K., Inoue, H., Kunieda, H., Iwasawa, K., 1995, MNRAS, 277, 901
Reynolds, C.S., Fabian, A.C., 1995, MNRAS, 273, 1167
Ross, R.R, Fabian, A.C., Young, A., 1999, MNRAS, 306, 461
Simpson, C., Ward, M., O'Brien, P.T., Reeves J.N., 1999, MNRAS, 303, L23
Stark A.A., et al., 1992, ApJS, 78, 77
Torres, C.A.O., et al., 1997, ApJL, 488, 19
Vaughan, S., Reeves, J., Warwick, R., Edelson, R., 1999a, MNRAS, 309, 113
Vaughan, S., Pounds, K.A., Reeves, J., Warwick, R., Edelson, R., 1999b, MNRAS, 308, L34
Voges, W. *et al.*, 1999, A&A, 349, 389
Zycki, P., Done, C., Smith, D.A., 1997, ApJ, 488, L113
Zycki, P., Krolik, J.H., Zdziarski, A.A., Kallman, T.R., 1994, ApJ, 437, 597

This paper has been produced using the Royal Astronomical Society/Blackwell Science LaTeX style file.